N79-16761

# SATURN'S ATMOSPHERE: RESULTS OF RECENT INVESTIGATIONS

**Laurence Trafton**

*University of Texas*
*Austin, Texas 78712*

**ABSTRACT**

We review recent developments in the study of Saturn's atmosphere. Saturn apparently has a high clear layer of $H_2$ under which lies a comparable layer rich in dusty material. Beneath this is a thicker layer consisting mostly of $H_2$ mixed with haze particles. An $NH_3$ cloud deck probably lies below this layer. Evidence for seasonal variations is presented in the form of changes in the $NH_3$, $CH_4$ and $H_2$ absorptions. Finally, the latest mixing ratios for the gaseous constituents are summarized.

## EXOSPHERE AND H TORUS

The extent of Saturn's atmosphere is uncertain. $L_\alpha$ emission has been observed from the OAO-C (Copernicus) satellite and a rocket to extend possibly out to Titan's radius. Barker (1977) reports $L_\alpha$ emission of 150 R with FWHM of 75 mÅ for a spectroscopic slit 0.3" × 39" projected on the torus region 5" to 10" inside Titan's orbital position. For Saturn's disk, he reports 250 R emission with FWHM of 100 mÅ. These observations were made during 12-15 April 1976 with OAO-C and are at the limit of photometric accuracy. The strengths are subject to revision depending on the concurrent geocoronal calibration.

Apparently, the first statistically significant detection of $L_\alpha$ emission from Saturn was obtained in March 1975 by Weiser, Vitz and Moos (1977) using a sounding rocket with circular spectroscopic apertures 26" and 53" in diameter. Saturn's disk had an angular extent of 17" by 19" and the outer edge of Ring A had an extent of 43" by 19". Assuming uniform emission intensity over the respective apertures, they derived a $L_\alpha$ brightness of 700 R ± 50 percent for Saturn's disk and 200 R ± 50 percent for the region outside and immediately adjacent to the disk, out to the radius of the large aperture. Any intensity distribution having zero emission from the region outside the disk is not compatible with the observations. The $L_\alpha$ brightness of Saturn's disk scales well with the 2 kR brightness for Jupiter, suggesting similar excitation mechanisms in the upper atmospheres of both planets (resonant scattering). Weiser *et al.* estimate only 10 R emission for H in the vicinity of the Rings from meteoroid bombardment of the Rings, solar and interstellar wind bombardment, and ice sublimation. Saturn's inclination is high enough so that any contribution of a H torus centered along Titan's orbit to the 200 R observed in the vicinity of the Rings would require ejection velocities of H from Titan nearly comparable to Titan's orbital velocity (5.6 km/s). In this case, many atoms would be escaping the Saturn system so the torus geometry might not be a valid description of the H distribution.

In April of 1977, Barker (1978) repeated his observations and found essentially the same disk intensity but detected no emission (less than 100 R) over the Rings. Therefore, the question of emission next to Saturn's disk, in the immediate vicinity of the Rings, remains open.

## IONOSPHERE

The structure of Saturn's ionosphere was recently considered by Capone *et al.* (1977) who included, for the first time, the heating of cosmic-ray ionization as well as that of the extreme ultraviolet radiation of the Sun. These effects are comparable in the outer atmospheres of the major planets beyond Jupiter if the surface magnetic field is 2 Gauss or less and where the insolation is relatively diluted. They neglected the photochemistry of $NH_3$ and the possible roles of neutral hydrocarbons higher than $CH_4$. They also neglected negative-ion chemistry and plasma diffusion. They performed their analysis for an isothermal stratosphere and also for Wallace's (1975) model atmosphere to bracket the temperature regime. The electron densities (the quantity most likely to be observed) are plotted in Figure 1 for both cases; the calculated positive ion densities are shown only for the isothermal case. Characteristic of these calculations are two peaks in the electron density, whose altitude separation is diagnostic of the temperature structure in the inversion regime. An occultation experiment with a space probe promises to be a useful tool for investigating the thermal inversion of Saturn's atmosphere.

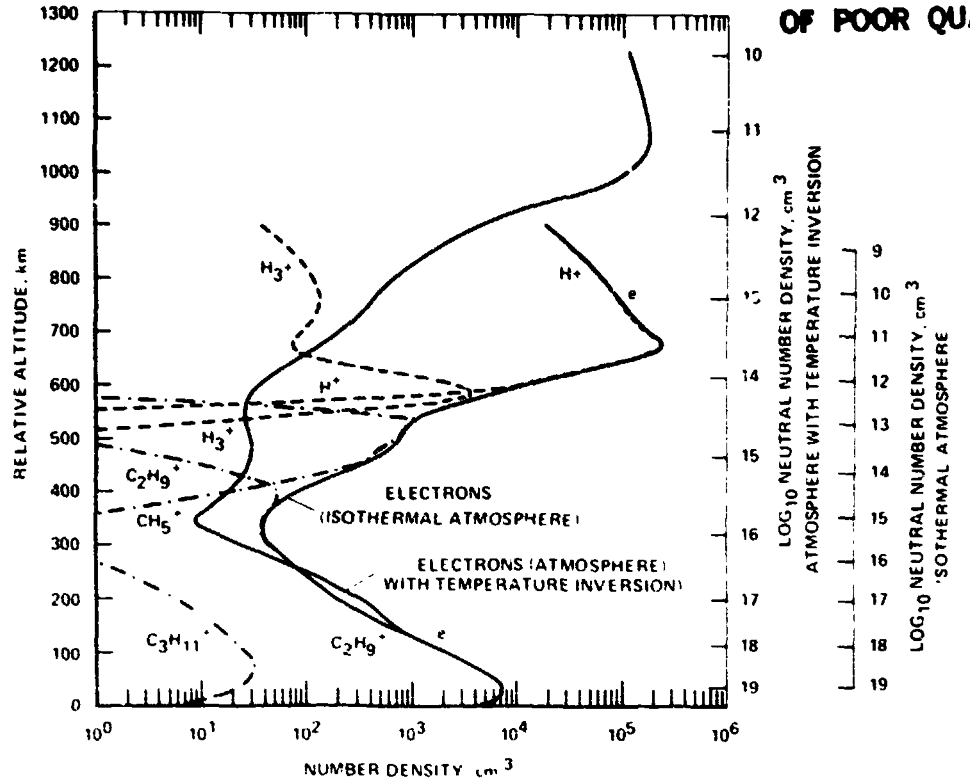


*Figure 1. Electron and ion number densities for Saturn. For purposes of clarity, the ion number densities are shown for the isothermal atmosphere only (Capone et al., 1977)*

TEMPERATURE INVERSION

The question of Saturn's atmospheric thermal structure in the lower inversion region and troposphere will be addressed at this workshop by Tokunaga, in addition to the question of the magnitude of Saturn's thermal flux. I will consider the aerosol structure and composition of Saturn's atmosphere and also the spatial and temporal variations. I will, therefore, confine this section to a few remarks.

The presence of Saturn's inversion layer was first indicated by the 7.5 - 13.4 $\mu$m observations of Gillett and Forrest (1974) at resolution $\lambda/\Delta\lambda$ = 67 (Figure 2). Their spectrum revealed an emission peak at 7.8 $\mu$m in the $\nu_4$ $CH_4$ band similar to that observed for Jupiter. The lack of a brightness temperature minimum around 8.2 $\mu$m indicates some unspecified extinction in Saturn's atmosphere which is not strong in

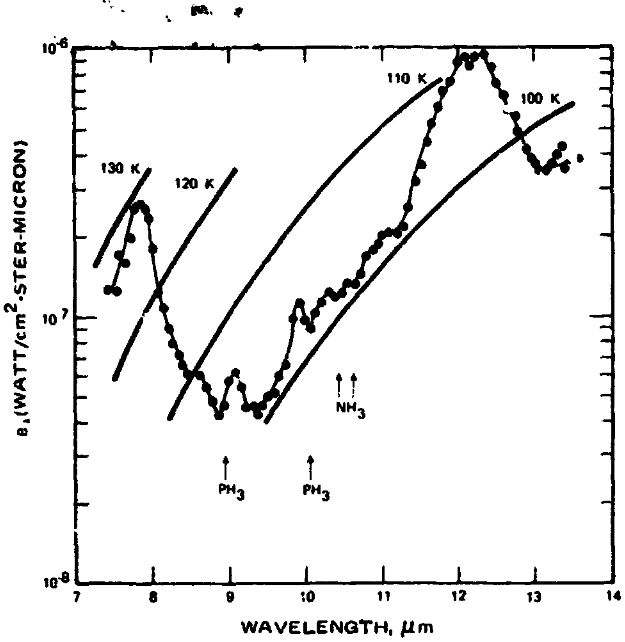


*Figure 2. Surface brightness of Saturn versus wavelength. Also shown are the locations of the Q branches of the $\nu_2$ and $\nu_4$ bands of $PH_3$. (Gillet and Forrest, 1974)*

Jupiter's atmosphere. They also detected the bright emission from the $\nu_9$ band of $C_2H_6$ centered around 12.2 $\mu$m. Soon thereafter, Gillett and Orton (1975) obtained several scans across the disk of Saturn at 11.7 $\mu$m ($\Delta\lambda$ = 0.18 $\mu$m) with a spatial resolution of 2".8 arc sec. These showed limb brightening, confirming the presence of a thermal inversion in Saturn's upper atmosphere. Observations using a broad band filter at 11.7 $\mu$m ($\Delta\lambda$ = 1.8 $\mu$m) showed less emission at the limb. These observations strongly support Danielson and Caldwell's suggestion that the emission arises from $C_2H_6$. They also found enhanced emission over the south pole (Figure 3), which they attribute to the increased insolation resulting from the tilt of this pole towards the Sun.

The thermal inversion affects the monochromatic flux primarily in the 7-20 $\mu$m spectral region. The continuum is cooler than the region of the inversion emitting hot radiation partly because the deep, hot region of the troposphere is hidden by the $NH_3$ haze in the spectral region where it is not effectively hidden by the pressure-induced $H_2$ opacity. The thermal inversion also tends to fill in the absorption features of the S(0) and S(1) pressure induced transitions of $H_2$, making the spectrum more like a black body. This filling in cannot be too strong, as in the case of Caldwell's (1977) model, because this would cause $H_2$ to radiate efficiently in the inversion zone. This would tend to destroy the inversion because a temperature inversion can only exist when there is no efficient radiator at thermal wavelengths in the inversion region to release the energy absorbed there from the solar heating of gas molecules and dust particles.

Figure 3. *Single polar scan at 11.7 μm through the pole. (Gillet and Orton, 1972).*

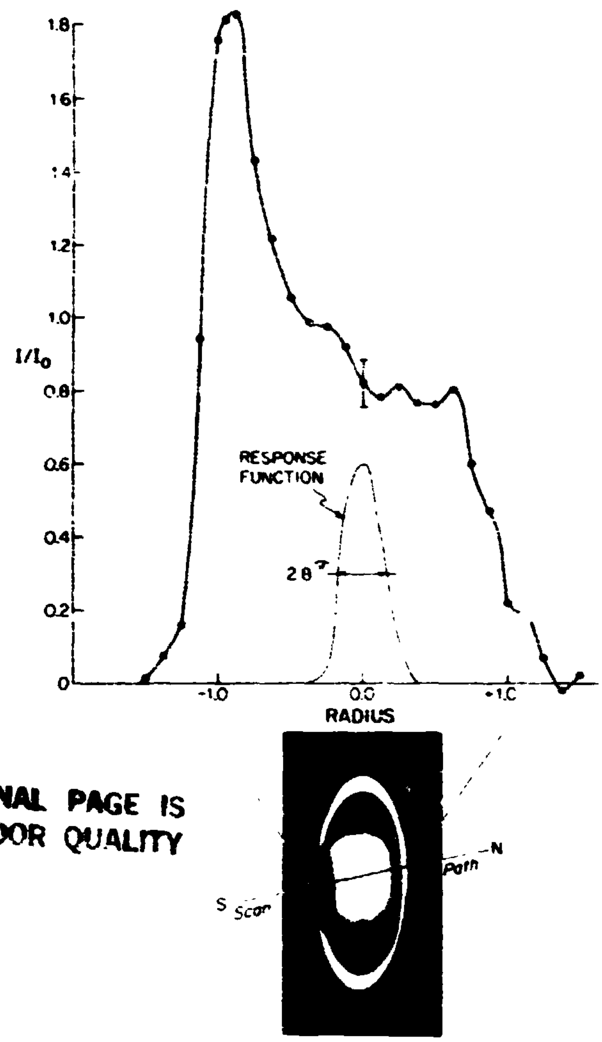




THE TROPOSPHERE AND $NH_3$ MIXING RATIO

Below the inversion region is the troposphere and associated haze layers and cloud decks. Below its sublimation level, $NH_3$ should be uniformly mixed with the other atmospheric bulk constituents. The microwave spectral observations permit the $NH_3$ distribution to be studied to depths much greater than for any other spectral region containing $NH_3$ bands. Several authors have *assumed* an isothermal stratosphere and convective troposphere in order to calculate synthetic spectra of the 1.25 cm $NH_3$ "inversion" band which they then compared with observations (Gulkis *et al.* 1969;

Wrixon and Welsh, 1970; Gulkis and Poynter, 1972). Models with solar $NH_3$ abundance below the saturation level and saturation values of the $NH_3$ partial pressure above the saturation level fitted the observations well. Ohring and Lacser (1976) dispense with the need for making these assumptions by using temperature profiles derived directly from inverting the emission spectrum of the 7.7 μm $CH_4$ band (Ohring, 1973), and using them to derive the $NH_3$ distribution directly from inverting the observed microwave emission spectrum. This spectrum they approximated by a smooth curve between 1 - 20 cm, using the points with higher signal to noise ratios. Their results, shown in Figure 4, depend on the $CH_4/H_2$ mixing ratio but are rather insensitive to the $He/H_2$ ratio for values $\leq 0.2$. For a nominal $CH_4/H_2 = 5 \times 10^{-4}$, they obtain a relatively constant value of $NH_3/H_2 = 1 \times 10^{-4}$ below the saturation level and, as for Jupiter (Ohring, 1973), they find $NH_3$ to be saturated (not supersaturated) above the saturation level. This level lies at 154 K and 4 atm for the nominal model. Its variation with $CH_4$ mixing ratio may be ascertained by reference to Figure 4.

Saturn's $NH_3$ abundance determined from the 6450 Å band has been relatively constant in the three year period ending 1975 (Woodman, Trafton and Owen, 1977). The abundance is 2 ± 0.5 m-am $NH_3$ "above the clouds" (equivalent reflecting layer model). Ohring and Lacser (1976) indicate that the level of line formation of $NH_3$ for an abundance of 2 m-am is above the highest level for which they have inferred $NH_3$ concentrations. The microwave results have the advantage that they pertain to much deeper layers than do the visual spectra.

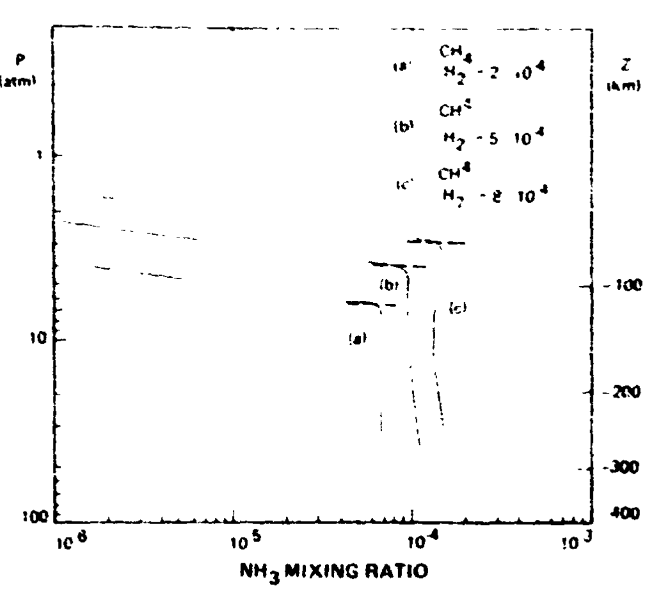


*Figure 4. Ammonia mixing ratio profiles for nominal temperature profile and for extreme temperature profiles. The level at which saturation begins is indicated by a dashed line (Ohring and Lacser, 1976).*

## HAZE

There appears to be an extended haze in Saturn's atmosphere near the 100-105 K levels. Gillett and Forrest's (1974) spectra show a brightness temperature in the 9-11 $\mu$m region of only 100-105 K, compared to ~130 K for Jupiter. They point out that this is too cold for the dominant gaseous opacity to be $NH_3$; the partial pressure of $NH_3$ in the layers responsible for Saturn's 9-11 $\mu$m emission is $10^{-2}$ to $10^{-3}$ times that in the layers responsible for Jupiter's 9-11 $\mu$m emission (which arises in the $\nu_2$ band of $NH_3$). My radiative convective models suggest that the top of Saturn's convective zone is at the 108-112 K level, well above the $NH_3$ saturation level, in contrast to Jupiter. If Saturn's haze consists of $NH_3$ particles suspended by convective currents, its extent in depth is much larger than for Jupiter. Caldwell (1977a) finds that indeed solid $NH_3$ crystals provide a good fit to Saturn's spectrum in the region of the 9.5 $\mu$m absorption feature visible in Gillett and Forrest's (1974) data. He also finds that the haze must be inhomogeneously distributed in depth, being concentrated at lower levels rather than mixed throughout the inversion. This haze layer is quite transparent at microwave wavelengths and is sufficiently thin at visual wavelengths that weak $NH_3$ lines are detectable in the 6450 Å band. Visible light penetrates below the 105 K level, where it undergoes multiple scattering.

The haze causes the subdued behavior of the equivalent widths of $H_2$, $CH_4$ and $NH_3$ from the center of the disk to the limb. The $H_2$ quadrupole lines are roughly constant over the disk; they are slightly stronger at the south pole and slightly weaker near the equatorial limbs (Trafton, 1972). The 6450 Å $NH_3$ band is strongest at the center of the disk, slightly weaker at the south pole, and quite weak near the equatorial limb (Woodman, Trafton and Owen, 1977) as indicated in Figure 5. Methane absorption is weaker in the equatorial belt and either about the same over the south pole and the center of the disk or slightly weaker over the pole (Teifel, Usoltseva and Kharitonova, 1971; 1973).

Saturn's limb darkening and polarization are not characteristic of pure Rayleigh scattering but of a haze with particles having an average radius of ~1 $\mu$m (Teifel, 1975).

The shapes of the R-branch manifolds of the 3 $\nu_3$ $CH_4$ band indicate the presence of some aerosol scattering (Trafton, 1973; Trafton and Macy, 1975; Macy, 1976) but they are much more compatible with a reflecting layer model (RLM) than a homogeneous scattering model. These observations were obtained along Saturn's central

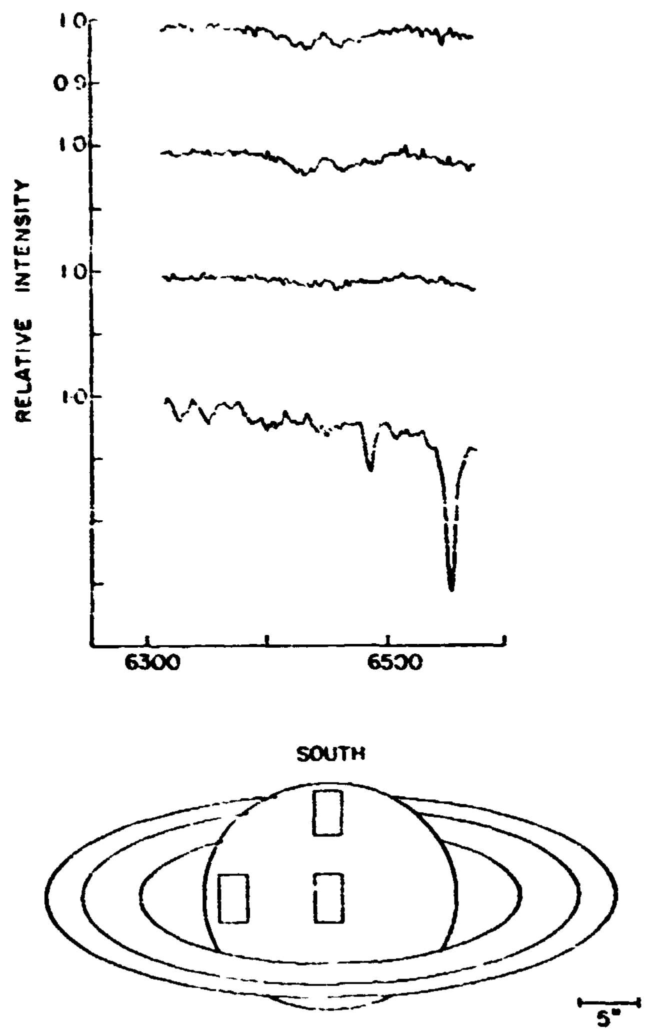


*Figure 5. Spatial variation of 6450 Å $NH_3$ band over the disk of Saturn, with ring spectrum for comparison. Size and placement of spectrograph slit are also illustrated. The top ratio spectrum corresponds to the south pole and the bottom one to the equatorial limb. (Woodman et al., 1977)*

meridian, excluding the equatorial belt and Rings. For this area, the RLM approximation may not be bad, at least in this wavelength regime. Figure 6a shows spatial scans I obtained along Saturn's central meridian at three wavelengths located in various $CH_4$ bands. They illustrate the $CH_4$ absorption increasing strongly towards the pole. Figure 6b shows the $CH_4$ absorption at these three wavelengths increasing toward the south pole.

Another manifestation of Saturn's haze is the lower abundance determinations in the infrared than in the visual spectrum (see the section below on Composition). Also, abundances determined from lines of very different strength at the same wavelength lead to conflicting values when analyzed in the RLM approximation. See de Bergh and Maillard (1977) for a discussion of this. Finally, we have already noted that the brightness temperatures at 8.2 $\mu$m and 9.5 $\mu$m indicate a haze.

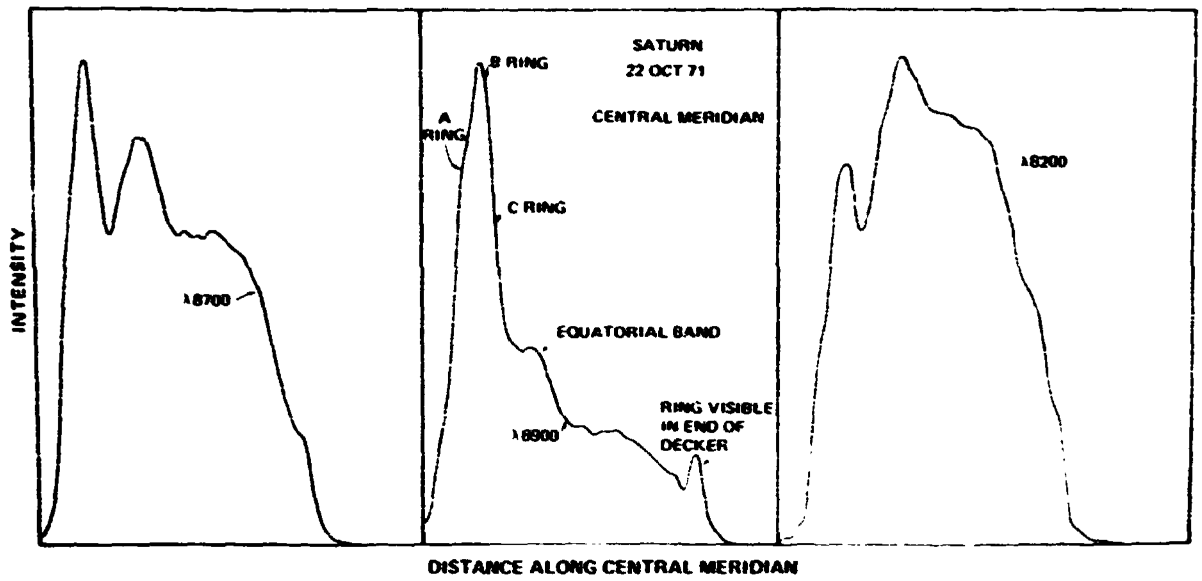


*Figure 6a. Spatial scans along Saturn's central meridian at three wavelengths in various $CH_4$ absorptions.*

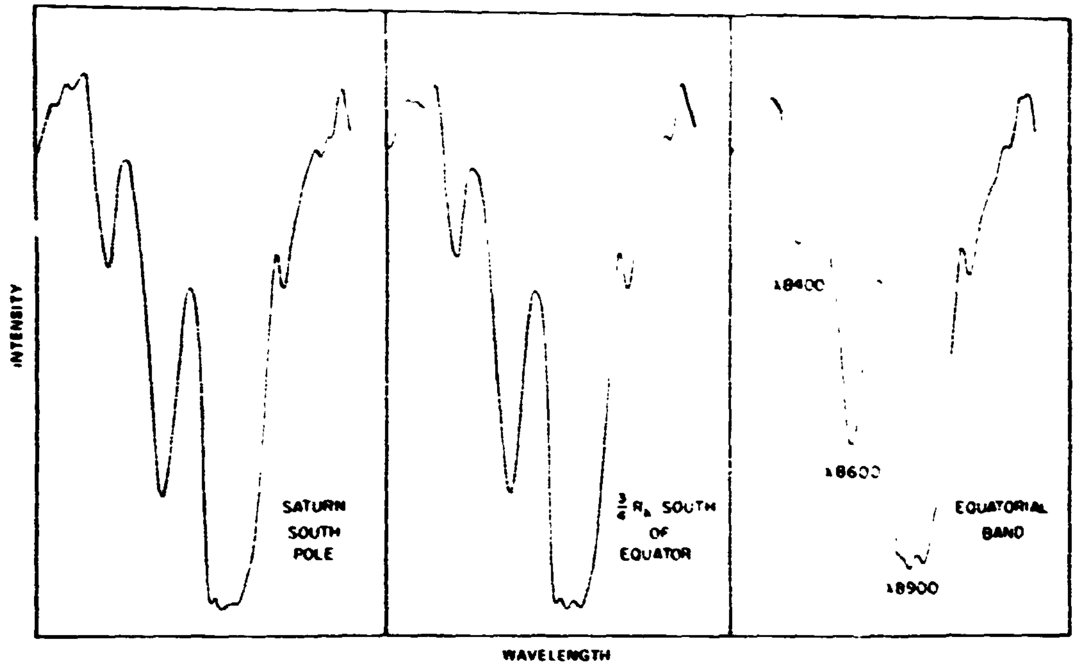


*Figure 6b. Spectral scans at three points along Saturn's central meridian covering the wavelengths of Fig. 6a.*

## DUST

The presence of dust in Saturn's atmosphere is deduced from the sharp drop in albedo between 5000 Å and 3000 Å. It probably arises from photochemistry of $CH_4$ photodissociation products (Caldwell, 1977a). Podolak and Danielson (1977) have modeled this albedo in terms of a homogeneous dust layer mixed with 28 km-A (kilometer-Amagat) $H_2$ above a cloud deck and under a clear layer $H_2$ 7 km-A thick. The parameters of the dust follow: The real part of the index of refraction = 2.0; the imaginary part $\sim \lambda^{-2.5}$; and a flat distribution in particle radii from 0 to 0.1 $\mu$m. The dust parameters are the same as those successfully used to model the blue-UV albedos of Jupiter and Titan. At 5000 Å, the optical depth for extinction of the dust is 0.7. The fit is shown in Figure 7. It should be noted that these models of the dust distribution are not unique. The effect of an inhomogeneous depth distribution of the dust would be to change the value of the exponent $\alpha$ in the imaginary part of the refractive index (Barker and Trafton, 1973).

The presence of a high, clear region of the atmosphere, free of dust and aerosol particles, is required by the increase in albedo shortwards of 3000 Å (cf. Figure 7). This occurs as a result of a sharply increasing cross section of Raleigh scattering. A layer of 7-28 km-A is needed, depending on the model. Podolak and Danielson (1977) place 7 km-A $H_2$ in the clear region; Teifel (1975) places "less than 13" km-A $H_2$ there; and Macy (1977) places 27 km-A $H_2$ there.

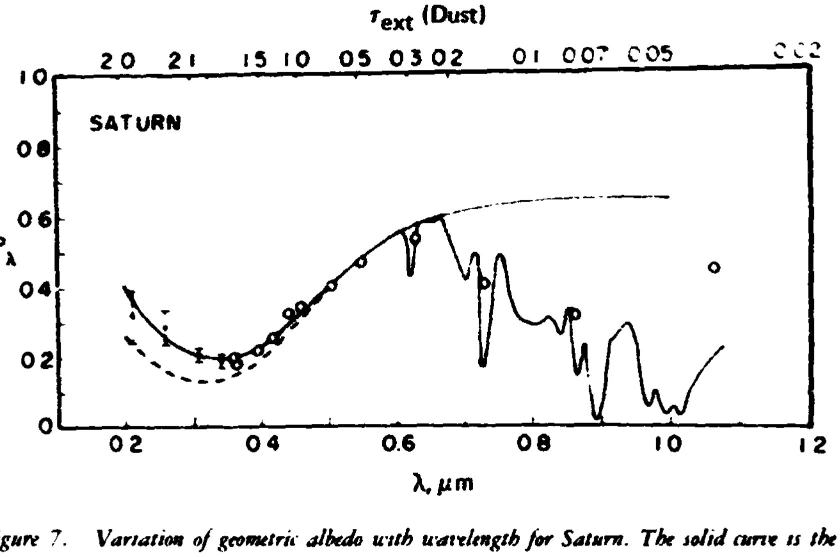


*Figure 7. Variation of geometric albedo with wavelength for Saturn. The solid curve is the theoretical fit to the data with a 7 km-am-region of $H_2$ above the dust. The dashed curve is the fit without such a clear layer. The methane absorptions are also shown. (Podalak and Danelson. 1977).*

More accurate modeling of this region is needed. The presence of limb brightening in the UV (Marin, 1968) also requires a relatively clear upper atmosphere. New measurements, such as those of Franz and Price (1977) may help the modeling. They find pronounced limb brightening in U, moderate limb brightening in B and limb darkening in V.

## AEROSOL STRUCTURE

The best model to date of Saturn's aerosol structure is Macy's (1977) but this model does not agree with all observations so there is room for improvement. For the thermal structure, Macy uses the temperature profile of Caldwell's thermal model (1977a) but adjusts the effective temperature to 97 K instead of 93.5 K and uses a surface gravity of 1050 cm $s^{-2}$. Caldwell's inversion region is too low for it causes $H_2$ to appear in emission in his model but this does not significantly affect the aerosol structure. The various models for the inversion converge in the troposphere although they disagree in the inversion regime. The convergence is a result of the $H_2$-He opacities being relatively well known because these opacities control the radiative transfer in the troposphere.

Macy's model is constructed to agree with photometric and spectroscopic data in the UV, visible and near IR while Caldwell's (1977a) thermal model is concerned with the spectral characteristics for wavelengths longer than 8 $\mu$m, except for solar heating. Scattering is not included in the radiative transfer of Caldwell's model but is included in Macy's model. Other differences are that Macy's model includes a clear region above the absorbing dust and has the cloud deck at the $NH_3$ sublimation level rather than at the radiative-convective boundary. The former is motivated by the UV limb brightening and rise in albedo. The latter is motivated by the visibility of weak gaseous $NH_3$ absorptions, relatively large $H_2$ equivalent widths and high rotational temperatures for $CH_4$. Macy's model also distinguishes the equatorial from the temperate zones, as indicated in Table 1.

Figure 8 shows Macy's schematic for Saturn's atmosphere. Above the opaque cloud deck is 52 km-A $H_2$ mixed with haze particles. Multiple scattering in this region enhances the equivalent widths of the $H_2$ lines but obscures the gaseous $NH_3$ absorption. Above the haze is a layer of absorbing particles (or dust) 15-23 km-A $H_2$ thick and above this there is the clear region 19-27 km-A $H_2$ deep. The dust layer accounts for the drop in albedo in the blue-UV spectral region and helps to heat the upper atmosphere. The

Table 1. Particle Distribution

| Layer | $H_2$ Abundance (km-A) | | Pressure at Layer Bottom, Equator (atm) | Pressure at Layer Bottom, Temperate (atm) |
|---|---|---|---|---|
| | Equator | Temperate | | |
| Clear gas | 19 | 27 | 0.2 | 0.3 |
| Absorbing Particle | 23 | 15 | 0.4 | 0.4 |
| Haze Particle | 52 | 52 | 1.1 | 1.1 |

haze layer also helps to explain the shapes of the $3\nu_3$ $CH_4$ manifolds and the low brightness temperature at 9.5 μm (but the cross section for the particles may be quite different at visual wavelengths than at 9.5 μm). Macy's model incorporates the Raleigh phase function for scattering by the gases and an isotropic phase function for scattering by the particles. The particle albedo is scaled according to the van de Hulst similarity relations to account for their anisotrapy. Because greater polarization is observed in the temperate region than in the equatorial belt, Macy argues that absorbing particles should lie deeper in the temperate region. His model is also constrained by molecular line observations: in particular, the (3-0) and (4-0) $H_2$ quadrupole lines, lines from the weak 6450 Å $NH_3$ band, and manifolds from the $3\nu_3$ $CH_4$ band R branch.

Macy's model fits the spectral reflectivity well (Figure 9). On the other hand, the fit of the reflectivity from the center of the disk to the equatorial limb is rather poor (see Figure 10). This is due in part to approximating anisotropic scattering by isotropic. There is also a problem with the high rotational temperature of the $3\nu_3$ $CH_4$ band. The high-J manifolds are too strong relative to those in his model. He discussed this problem in a previous paper (Macy, 1976) which analyzed the $3\nu_3$ $CH_4$ band and $H_2$ absorptions simultaneously using an inhomogeneous model atmosphere. He found that if the

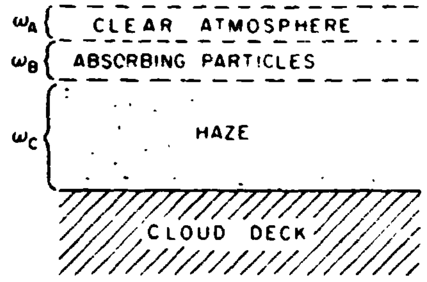


*Figure 8. Diagram of the model. Values for the $H_2$ abundance in the clear layer, $\omega_a$, the absorbing particle layer, $\omega_b$, and the haze layer, $\omega_c$, are given in Table I. The absorbing particle-haze layer boundary corresponds to the radiative-convective boundary. The bottom of the cloud deck is at the ammonia sublimation level.*

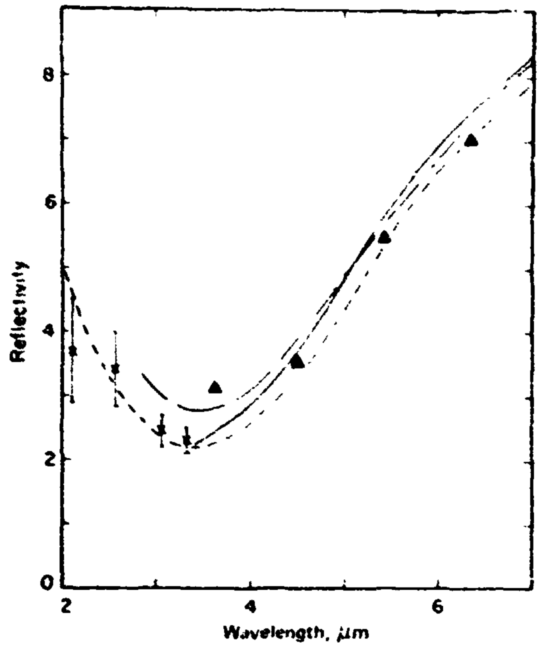


*Figure 9. Observed reflectivity as a function of wavelength in the equatorial region (solid line), the temperate region (at latitude 40°S in the south temperate zone (Rose, 1971)) (triangles), and OAO II geometric albedo (Caldwell, 1975), which have been increased by 20% to give an estimated equatorial reflectivity (error bars). Calculated reflectivities are for the equatorial region (R/R(planet) = 0.0) (long-dashed line) and the temperate region (R/R(planet) = 0.4) (short-dashed line).*

*Figure 10. Observed reflectivity along the equator normalized to unity at the center of the disk (Martin, 1968), at 6250 Å (short-dashed line) and 3550 Å (dash-dot line). Calculated reflectivity at 6250 Å (long-dashed line) and 3550 Å (solid line). The theoretical curves have not been convolved with a point spread function. A full treatment of the limb darkening must take into account the anisotropy of the scattering phase function and smearing due to seeing.*

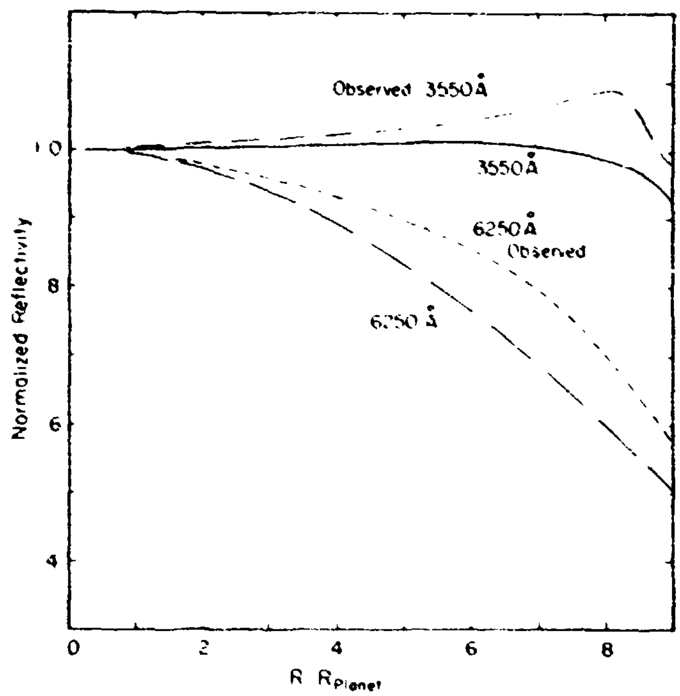


optical thickness of the haze layer was adjusted to fit the observed $H_2$ absorption, the effective depth of absorption for the $3\nu_3$ $CH_4$ band was so shallow that the rotational temperature of the band came out too low.

It seems to me that this problem could be resolved if the mean cross section of the haze particles in his model were allowed to decrease with increasing wavelength rather than be held constant. This variation is required to explain the (3-0) and (4-0) $H_2$ absorptions in Uranus' atmosphere (Trafton, 1976). Then deeper, hotter layers would contribute to the $3\nu_3$ $CH_4$ absorption at 1.1 µm while shallower layers limit the

$H_2$ absorption at 0.64 $\mu$m and 0.82 $\mu$m. This modification should also result in a revision of the derived $CH_4/H_2$ ratio.

Finally, there appears to be some uncertainty about the depth of the $NH_3$ sublimation level. Macy's model gives 1.1 atm but that derived from inversion of the $NH_3$ microwave spectrum (Ohring and Lacser, 1976) is 4 atm for a $CH_4/H_2 = 5 \times 10^{-4}$. Macy's model has four times the methane mixing ratio. The microwave results are brought into closer agreement with Macy's sublimation level if Macy's methane mixing ratio is assumed. This would require a larger $NH_3$ mixing ratio, however, so the depth, at present, must be considered uncertain.

## SEASONAL VARIATIONS

Spectra of $H_2$, $NH_3$ and $CH_4$ obtained over a long time base indicate that significant seasonal variations occur. The visibility of the 6450 Å $NH_3$ band has ranged from zero to almost the strength of Jupiter's band. Dunham (1933) was able to see as many lines of this band in Saturn's spectrum as he saw in Jupiter's spectrum. This is not surprising in view of the exponential dependence of the equilibrium $NH_3$ vapor pressure on the temperature and the deep $NH_3$ haze layer. Small changes in temperature could cause much bigger changes in the $NH_3$ visibility.

Observations of the $H_2$ quadrupole lines over the past decade are shown in Figure 11 (Trafton, 1976) and indicate a seasonal variation correlated with the shading of the planet's disk by the Rings. Figure 12 shows more recent data for strong $CH_4$ bands. If the trend given by the earlier $H_2$ points is correct, Saturn's atmosphere mimics the deep, clear atmosphere of Uranus at a time when the Rings are edge on (minimum shading) which also happens to be when the planet is farthest from the Sun. The Ring shading and orbital eccentricity each produce 15% variations in the insolation of the disk. The $H_2$ equivalent widths appear to be minimum at the time of maximum shading, suggesting a lot of haze opacity in the deeper atmosphere. The $CH_4$ bands, which probe shallower regions of Saturn's atmosphere, show a recent increase in strength, suggesting that haze may be settling out of Saturn's upper atmosphere after the time of maximum Ring shading. Further monitoring of Saturn's $H_2$, $NH_3$ and $CH_4$ absorption is needed to confirm the seasonal behavior and to understand its causes. The scatter of the points in Figure 11 indicates that the diurnal and short term variations are typically less than 10%.

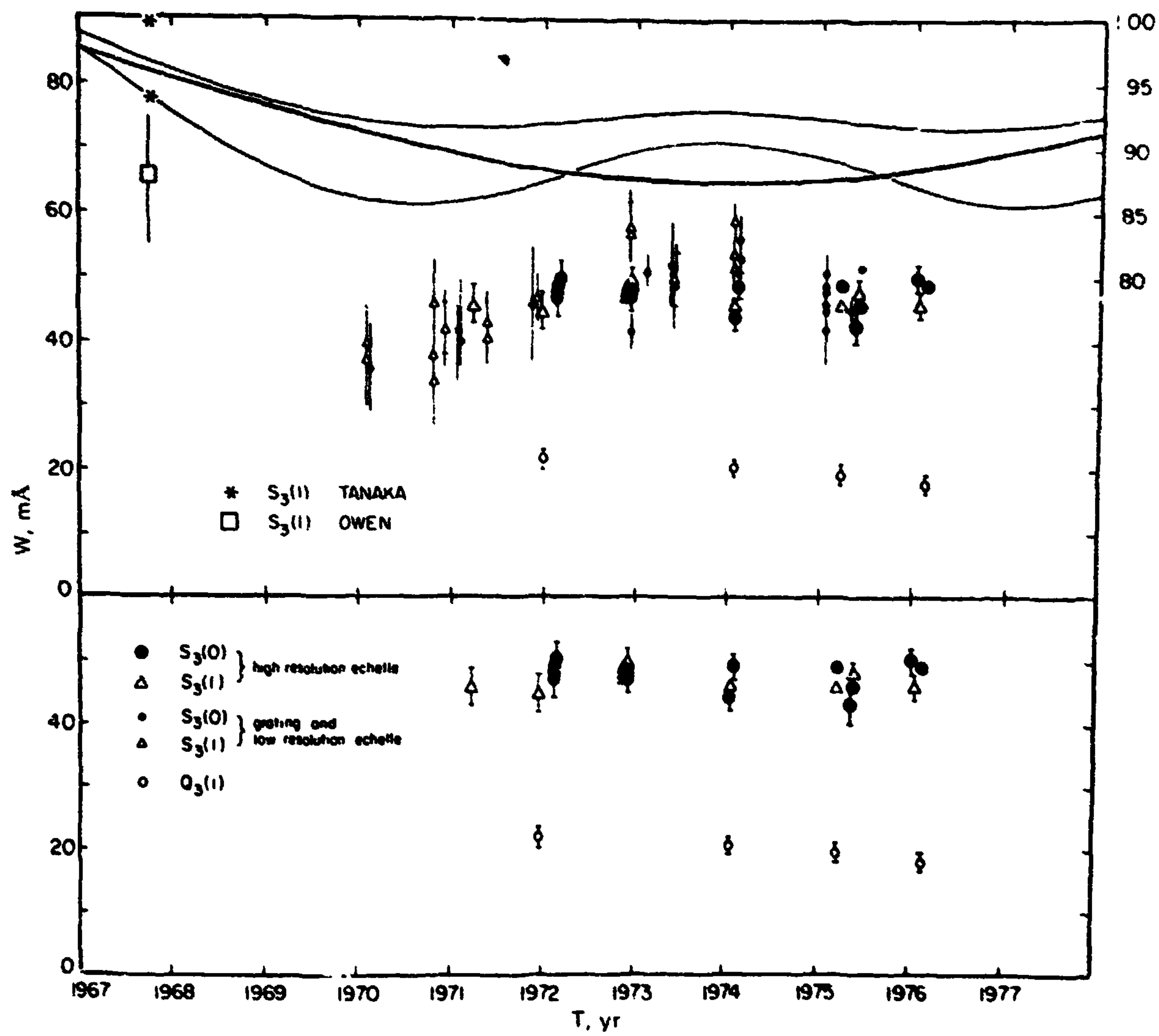


*Figure 11* Time variation of $H_2$ equivalent widths. The long term behavior is presumably seasonal. An upper limit to the diurnal behavior is given by the scatter. (a) Values from all spectra. The wavelength scale on the right is for the curves at the top of the figure. The heavy curve describes the square of Saturn's distance from the Sun normalized to unity in January 1966. It was maximum in May of 1959. It is inversely proportional to the insolation. The light curves bracket the fractional shading of Saturn's disk by the rings. The absorption was minimum at the time the shading of the rings was maximum. When shading was minimal, the $H_2$ absorption may have been greatest when Saturn was farthest from the Sun. Near this time, the depth of the $NH_3$ cloud should have been greatest. (b) Values from the high-resolution spectra alone. These have a lower scatter and are less susceptible to errors resulting from blended telluric $H_2O$ lines. Encrenaz and Owen (1973) measured values in February of 1973 for the (3−0) lines. Their value for $S_3(0)$ agrees with our data well but their value (41 + [illegible] mÅ) for $S_3(1)$ is 15% lower.

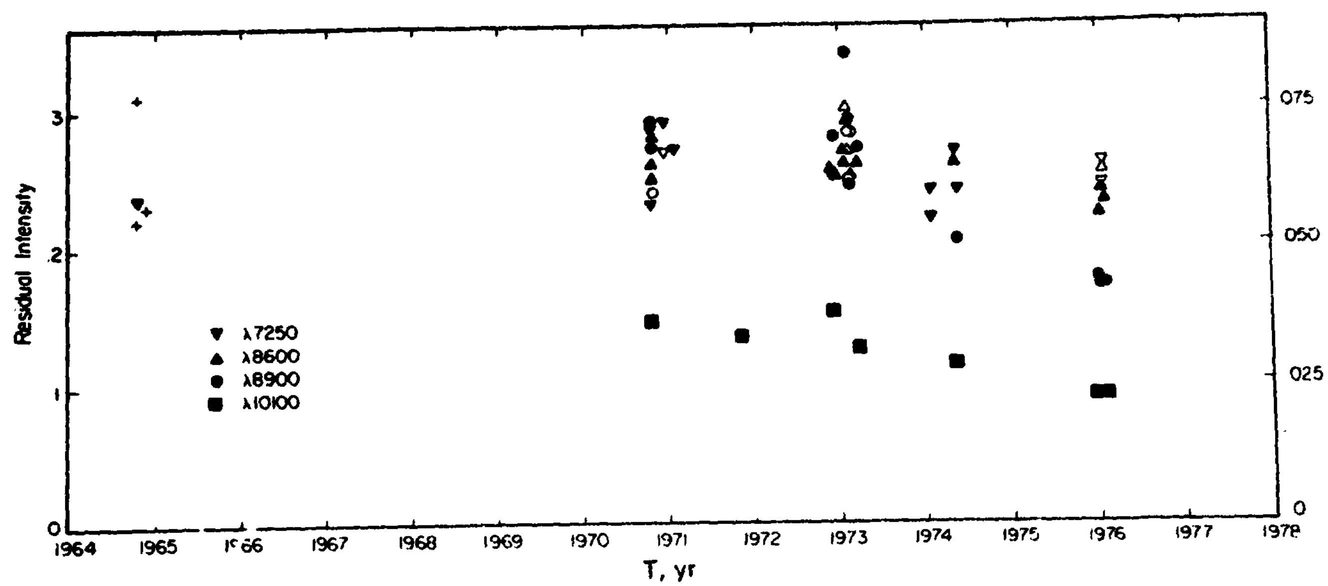


*Figure 12.* *Long-term variation of Saturn's $CH_4$ absorption on the central meridian, excluding the equatorial belt and the hemisphere shaded by the rings. The precise wavelengths are shown in Figure 5. The scale on the right is for the λ 8900 band's residual intensity. The scale on the left is for the other three bands. The uncertainty of the values from the λ 10 100 band is equal to the height of the symbol. These points have the highest accuracy owing to no blending with telluric $H_2O$ and a fairly wide band minimum. The uncertainty of the other values is best estimated from their scatter. The open symbols indicate greater measurement uncertainty. The + symbol plots points taken with the slit set parallel to Saturn's equator in the northern hemisphere during 1964. All bands indicate an increase in absorption.*

COMPOSITION

The questions of composition are what gases compose Saturn's atmosphere and what are their relative abundances? In addition to $H_2$, $NH_3$ and $CH_4$; detected gases include H (Weiser *et al.*, 1977), $^{13}CH_4$ (Combes *et al.*, 1975), HD (Smith and Macy, 1977; Trauger, Roesler and Mickelson, 1977), $C_2H_6$ (Tokunaga, Knacke and Owen, 1975), $PH_3$ and $CH_3D$ (Fink and Larson, 1977). Helium has not yet been detected; its presence is inferred from cosmogony and possibly from the shape of the thermal spectrum. Solid $NH_3$ appears to be responsible for the absorption at 9.5 $\mu m$ and possibly at 8.98 $\mu m$ (Caldwell, 1977a). There appears to be a weak feature at 10.1 $\mu m$ in the spectra of Gillett and Forrest (1974) which might arise from solid $NH_2D$ (Caldwell, 1977) but higher resolution spectra are needed to confirm this possibility.

The controversy on whether the features at 10-11 $\mu m$ are due to $PH_3$ (Bregman *et al.*, 1975) or to $C_2H_4$ (Encrenaz *et al.*, 1975) appears to be resolved in favor of $PH_3$ since Fink and Larson (1977) have detected $PH_3$ in Saturn's 5 $\mu m$ spectrum. They find the absorption to be considerably stronger than on Jupiter. About 50 cm-A of laboratory $PH_3$ is needed to match the broad $PH_3$ feature at 4.73 $\mu m$. These authors also find the Q and P branches of $CH_3D$ to be quite prominent in Saturn's spectrum and the line strengths are comparable to those of $CH_3D$ on Jupiter. About 5 cm-A of laboratory $CH_3D$ is needed to match their absorption. Smith and Macy (1977) derive a value for $D/H = (6.6 \pm 3.1) \times 10^{-5}$ from the $R_5(0)$ line of HD and Trauger *et al.*, (1977) report a similar value $(5.1 \pm 0.7) \times 10^{-5}$ from the $P_4(1)$ line of HD. Modeling the emission from the $\nu_9$ band of $C_2H_6$ at 12.2 $\mu m$, Caldwell (1977a) estimates a mixing ratio $C_2H_6/H_2 = 1.8 \times 10^{-6}$.

A number of abundances for $H_2$, $NH_3$ and $CH_4$ have been given in the literature in the reflecting layer approximation. For the (3-0) and (4-0) $H_2$ quadrupole lines, Encrenaz and Owen (1973) quote 77 ± 20 km-A $H_2$ using the curve of growth of Fink and Belton (1969) which is now outmoded because the pressure broadening coefficients have since been improved (Macy, 1973). For the $Q_2(1)$ line, de Bergh *et al.* (1977) obtain a $H_2$ abundance of $25^{+9}_{-6}$ km-A also by using Fink and Belton's curve of growth. For the pressure-induced fundamental, Martin derived $25^{+10}_{-9}$ km-am $H_2$ with a base temperature of 150 K and a base density of $0.52^{+0.26}_{-0.17}$ amagats. For the first overtone of the pressure-induced $H_2$ band, Lecacheux *et al.* (1976) derived $63^{+13}_{-8}$ km-A $H_2$. From the 6450Å $NH_3$ band, Woodman *et al.* (1977) derived 2.0 ± 0.5 m-A $NH_3$.

But from the 1.56 $\mu$m $NH_3$ band, Owen *et al.* (1976) derived an upper limit of 0.15 m-A. Using the $3\nu_3$ $CH_4$ band, Trafton (1973) derived a $CH_4$ abundance of $54 \pm 13$ m-A (Trafton and Macy, 1975) and Lecacheux *et al.* (1976) derived $59^{+15}_{-7}$ m-A. On the other hand, Lutz *et al.* (1976) analyzed the weak blue and green bands and derived ~150 m-A $CH_4$.

It is easily seen from this that the abundances derived in the RLM approximation vary both with the wavelength of the band analyzed and with the strength of that band. Except perhaps for the central meridian, the RLM approximation is probably poor. Even comparing bands at the same wavelength but of different strengths requires that the radiative transfer include scattering. Meaningful abundance ratios may be obtained without analysis of the radiative transfer if absorption features of the two gases in question can be found and measured which have comparable strengths (de Bergh and Maillard, 1977). This ratio is independent of the radiative transfer, at least for weak lines. Therefore, duplicating these absorptions with cold laboratory spectra yields the abundance ratio. This method has been applied successfully for C/H and $^{12}C/^{13}C$ in the atmospheres for Jupiter and Saturn. For Saturn, Lecacheux *et al.* (1976) derive C/H = $4.7^{+2.0}_{-1.3} \times 10^{-4}$ and Combes *et al.* (1977) derive $89^{+25}_{-18}$, respectively. Figure 13 shows several manifolds of Saturn's $^{13}CH_4$ spectrum and the



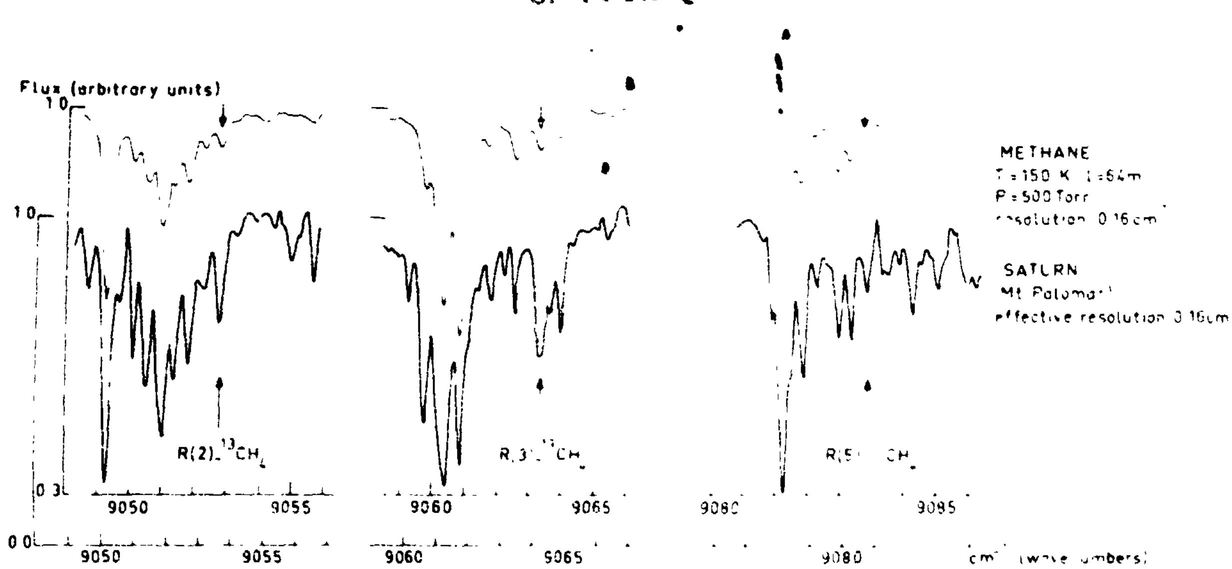


*Figure 13. Lower curve. Portions of a spectrum of Saturn recorded at Mt. Palomar in 1974 with a Connes interferometer. Resolution for planetary lines: 0.16 cm$^{-1}$ S/B (B=2σ)=2... Upper curve Portions of a laboratory spectrum of $CH_4$ (as in Figure 1). The spectral resolution has been degraded to 0.15 cm$^{-1}$ for a better comparison with the Saturn spectrum (Combes et al., 1977).*

laboratory $CH_4$ features used to compa them. These values are essentially the same as the solar values, and the same as the telluric value in the case of $^{12}C/^{13}C$.

Podolak and Danielson (1977) have shown the importance of including dust and haze in determining abundances from atmospheric models. They were successful in constructing such models which give both the observed absorptions for the weak blue bands of $CH_4$ and the stronger bands the red and near infrared.

Some results for the $CH_4/H_2$ mixing ratio from such models follow: Podolak and Danielson (1977); 5x solar C/H ($CH_4/H_2 = 3.5$ to $3.9 \times 10^{-3}$); Caldwell (1977a): 4.7x solar ($CH_4/H_2 = 2.1 \times 10^{-3}$); Mach (1977): ~.5x solar. These are all higher than the value of Lecacheux *et al.* (1976), who derive approximately the solar ratio. This discrepancy requires further study.

Saturn's UV spectrum obtained by the TD1a and OAO-2 satellites shows no definite absorption features (Caldwell, 1977b). Saturn's albedo from 2100Å to 2500Å is similar to Jupiter's, implying that there is a common UV absorber. This absorber cannot be $NH_3$ on either planet because it is frozen out to much deeper levels in Saturn's atmosphere so that it should affect Saturn's spectrum differently. Caldwell (1977b) models the $H_2S$ absorption and finds that a mixing ratio of $H_2S/H_2 = 1.4 \times 10^{-8}$ fits Saturn's UV spectrum (see Figure 14). This compares with the upper limit of $4 \times 10^{-7}$ on this mixing ratio reported by Owen *et al.* (1976) for Saturn from the 6289 $cm^{-1}$ band. Caldwell's value is much less than the corresponding solar S/H ratio, implying that S is bound in other molecules.

Scattergood and Owen (1977) consider the composition of the blue-UV "dust" in terms of the production of organics by proton bombardment of $H_2$, $CH_4$ and $NH_3$ mixtures. Their results show that $CH_4+H_2$ mixtures remain clear but the addition of N (e.g. $NH_3$) or S (e.g., $H_2S$) leads to the production of colorful liquids and solids. None has the spectral behavior identical to those shown by the planets so mixtures would be required to explain the haze. As yet, there is no satisfactory explanation for what material is causing the absorption between 5000-3000 Å in Jupiter, Saturn or Titan. This remains a major unsolved problem.

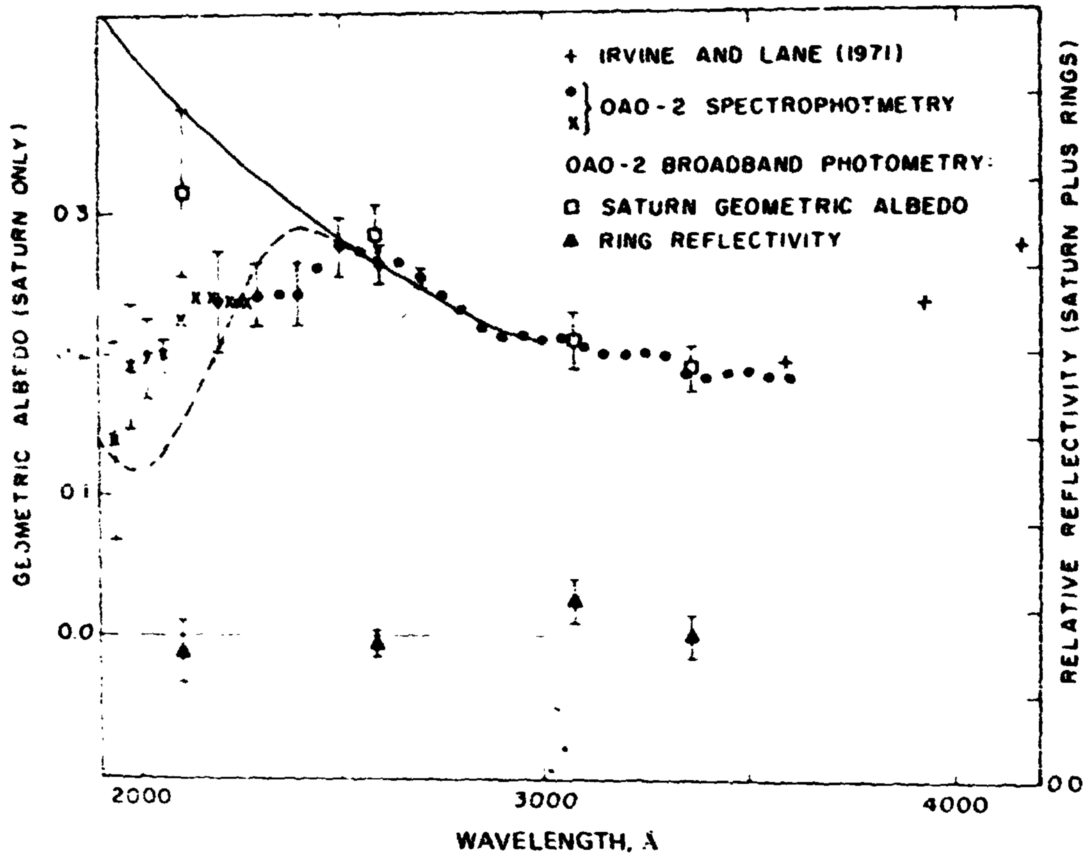


*Figure 14. Ultraviolet spectrophotometry of the Saturn system. The observational points (X, ●, +) are described by the right hand ordinate, which is the ratio of the brightness of the planet plus rings divided by the Sun. Regular OAO-2 spectrophotometry (ɸ), replotted from WCS, and long integration time spectrophotometry (ẋ), are shown with error bars only due to background uncertainty. The ring reflectivity (▲) error bars are due only to the uncertainty in extrapolating the total brightness to zero ring inclination. The Saturn geometric albedo points (Φ) were used to normalize the geometric albedo scale on the left. This scale is valid only shortward of 3500 Å. The solid curve is a model calculation including absorption by a trace amount of $H_2S$ (Caldwell, 1977b).*

## REFERENCES


Barker, E. (1977). Progress Report Copernicus observations of solar system objects. *Bull. Amer. Astron. Soc.* 9, 456.

Barker, E. (1978) Private communication

Barker, E., and Trafton, L. (1973). Ultraviolet reflectivity and geometric albedo of Titan. *Icarus* 20, 444–454.

Bregman, J., Lester, D., and Rank, D. (1975) Observation of the ν2 band of $PH_3$ in the atmosphere of Saturn. *Astrophys. J.* 202, L55–L56

Caldwell, J. (1977a) The atmosphere of Saturn, an infrared perspective. *Icarus* 30, 493–510

Caldwell, J. (1977b). Ultraviolet observations of Mars and Saturn by the TD1A and OAO-2 satellites. *Icarus* 32, 190–209.

Capone, L., Whitten, R., Prasad, S., and Dubach, J. (1977) The ionospheres of Saturn, Uranus, and Neptune. *Astrophys. J.* 215, 977–983.

Combes, M., Maillard, J., and deBergh, C. (1977) Evidence for a telluric value of the $^{12}C/^{13}C$ ratio in the atmospheres of Jupiter and Saturn. *Astron. Astrophys.* 61, 531–537

deBergh, C., Lecacheux, J., and Maillard, J. (1977) The 2-0 quadrupole spectrum of $H_2$ in the atmospheres of Jupiter and Saturn. *Astron. Astrophys.* 56, 227–233

# REFERENCES (Contd)


deBergh, C., and Maillard, J. (1977). Abundances from near infrared spectroscopy (in the giant planets). In *Proceedings of Symposium on Planetary Atmospheres* (A. V. Jones, ed.), pp. 9–18, Ottawa.

Dunham, T., Jr. (1933). Note on the spectra of Jupiter and Saturn. *Publ. Astron. Soc. Pac.* 45, 42–44.

Encrenaz, Th., and Owen, T. (1973). New observations of the hydrogen quadrupole lines on Saturn and Uranus. *Astron. Astrophys.* 28, 119–124.

Encrenaz, Th., Combes, M., Zeau, Y., and Vapillon, L. (1975). A tentative identification of $C_2H_4$ in the spectrum of Saturn. *Astron. Astrophys.* 42, 355–356.

Fink, U., and Belton, M. (1969). Collision-narrowed curves of growth for $H_2$ applied to new photoelectric observation of Jupiter. *J. Atmos. Sci.* 26, 952–962.

Fink, U., and Larson, H. (1977). The 5 μm spectrum of Saturn. *Bull. Amer. Astron. Soc.* 9, 535.

Franz, O., and Price, M. (1977). UBV pinhole scans of Saturn's disc. *Bull. Amer. Astron. Soc.* 9, 535.

Gillett, F., and Forrest, W. (1974). The 7.5 to 13.5 micron spectrum of Saturn. *Astrophys. J.* 187, L37–L38.

Gillett, F., and Orton, G. (1975). Center-to-limb observations of Saturn in the thermal infrared. *Astrophys. J.* 195, L47–L49.

Gulkis, S., McDonough, T., and Craft, H. (1969). The microwave spectrum of Saturn. *Icarus* 10, 421–427.

Gulkis, S., and Poynter, R. (1972). Thermal radio emission from Jupiter and Saturn. *Phys. Earth Planet. Interiors* 6, 36–43.

Lecacheux, J., deBergh, C., Combes, M., and Maillard, J. (1976). The C/H and $^{12}CH_4/^{13}CH_4$ ratios in the atmospheres of Jupiter and Saturn from 0.1 $cm^{-1}$ resolution near-infrared spectra. *Astron. Astrophys.* 53, 29–33.

Lutz, B., Owen, T., and Cess, R. (1976). Laboratory band strengths of Methane and their application to the atmospheres of Jupiter, Saturn, Uranus, Neptune, and Titan. *Astrophys. J.* 203, 541–551.

Macy, W. (1973). Inhomogeneous models of the atmosphere of Saturn. Ph.D. Thesis, Princeton University, 70 pp.

Macy, W. (1976). Analysis of Saturn's methane 3 $\nu_3$ band profiles in terms of an inhomogeneous atmosphere. *Icarus* 29, 49–56.

Macy, W. (1977). Inhomogeneous models of the atmosphere of Saturn. *Icarus* 32, 328–347.

Marin, M. (1968). Photometric photographique de Saturne. *J. Obs.* 51, 179–192.

Ohring, G. (1975). The temperature profile in the upper atmosphere of Saturn from inversion of the thermal emission observations. *Astrophys. J.* 195, 223–225.

Ohring, G., and Lacser, A. (1976). The ammonia profile in the atmosphere of Saturn from inversion of its microwave emission spectrum. *Astrophys. J.* 206, 622–626.

Owen, T., McKellar, A., Encrenaz, Th., Lecacheux, J., deBergh, C., and Maillard, J. (1977). A study of the 1.56 μm $NH_3$ band on Jupiter and Saturn. *Astron. Astrophys.* 54, 291–295.

Podolak, M., and Danielson, R. (1977). Axel dust on Saturn and Titan. *Icarus* 30, 479–492.

Scattergood, T., and Owen, T. (1977). On the sources of ultraviolet absorption in spectra of Titan and the outer planets. *Icarus* 30, 780–788.

Smith, W., and Macy, W. (1977). Observation of HD on Saturn and Uranus. *Bull. Amer. Astron. Soc.* 9, 516.

Teifel, V. (1975). Limb darkening on Saturn's disc. *Astron. Zh.* 52, 823–831.

Teifel, V., Usoltseva, L., and Kharitonova, G. (1971). Optical properties and structure of Saturn's atmosphere. I. Preliminary results of studies of $CH_4$ absorption bands on the planetary disc. *Sov. Astron.* 15, 296–302.

Teifel, V., Usoltseva, L., and Kharitonova, G. (1973). Optical properties and structure of Saturn's atmosphere. II. Latitudinal variations of absorption in the 0.62-μm $CH_4$ band and characteristics of the planet in the near ultraviolet. *Sov. Astron.* 17, 108–111.

Tokunaga, A., Knacke, R., and Owen, T. (1975). The detection of ethane on Saturn. *Astrophys. J.* 197, L77–L78.

Trafton, L. (1972). Quadrupole $H_2$ absorption in the spectra of Jupiter and Saturn. *Bull. Amer. Astron. Soc.* 4, 359.

Trafton, L. (1973). Saturn: A study of the 3 $\nu_3$ methane band. *Astrophys. J.* 182, 615–636.

Trafton, L. (1976). The aerosol distribution in Uranus' atmosphere: Interpretation of the hydrogen spectrum. *Astrophys. J.* 207, 1007–1024.

Trafton, L. (1977). Saturn: Long-term variation of $H_2$ and $CH_4$ absorptions. *Icarus* 31, 369–384.

Trafton, L., and Macy, W. (1975). Saturn's 3 $\nu_3$ methane band: An analysis in terms of a scattering atmosphere. *Astrophys. J.* 196, 867–876.

Trauger, J., Roesler, F., and Mickelson, M. (1977). The D/H ratios on Jupiter, Saturn, and Uranus based on new HD and $H_2$ data. *Bull. Amer. Astron. Soc.* 9, 516.

Wallace, L. (1975). On the thermal structure of Uranus. *Icarus* 25, 538–544.

Weiser, H., Vitz, R., and Moos, H. (1977). Detection of Lyman α emission from the Saturnian disk and from the ring system. *Science* 197, 755–757.

Woodman, J., Trafton, L., and Owen, T. (1977). The abundances of ammonia in the atmospheres of Jupiter, Saturn, and Titan. *Icarus* 32, 314–320.

Wrixon, G., and Welch, W. (1970). The millimeter wave spectrum of Saturn. *Icarus* 13, 163–172.

## DISCUSSION

J. CALDWELL: Concerning the controversy over ethylene and phosphine at 10.5 μm, I don't think that the observations of Fink and Larson rule out ethylene. If ethylene is being seen at that wavelength, it's in emission at a very high altitude. And if that were true, you would see emission from ethylene on top of any possible absorption by phosphine so that, in fact, both observations could be right; they're not mutually exclusive.

L. TRAFTON: The observations of Fink and Larson show that the phosphine is fairly strong, stronger than in Jupiter, so it would also be absorbing in the 9 to 10 μm region fairly strongly.

J. CALDWELL: But if ethylene is emitting above that, you see the ethylene.

G. SISCOE: Do the Copernicus Lyman-alpha measurements give a density value or a density limit for the Titan torus?

L. TRAFTON: They give an intensity of about 150 Rayleighs for the Titan torus. E. Barker (1977) pointed out from OAO data, that within ten arc-sec of Titan a 39-arc-sec measurement gave about 150 Rayleighs, which would be a limit for their detection. And when he looked again, I believe he saw about the same number.

J. POLLACK: When you speak about the observations of the Titan torus, is that a discrete torus?

L. TRAFTON: The observations are made through a 39-sec slit superimposed over the torus about five or ten-sec away from Titan. I understand there is a problem with the geocoronal calibration of atomic hydrogen data. That has to be subtracted out, and you're subtracting two large numbers which are roughly equal to each other and in that circumstance, there can be large uncertainties. It's a difficult problem and I think even more observations are needed to convince a majority of the community one way or another whether the hydrogen emission really is present at all, to say nothing of the detailed geometry.

D. HUNTEN: You were praising the use of spectral features of comparable strengths in getting relative abundances, but there's another important point that I've recently become sensitive to: you want comparable physics as well. You don't want to compare a pressure-induced feature with a pressure-narrowed feature, for example, if you can possibly help it, because every time the physics is different like that, you have a different depth weighting in the formation of the spectral feature. You must go a lot further than just to look for comparable features, and unfortunately, in comparing hydrogen and methane, nothing is really comparable. Every time you look for a useful pair, you find that the depth weighting is totally different.

L. TRAFTON: Unfortunately, I have to agree.